PCCP
Physical Chemistry Chemical Physics

Accepted Manuscript

This article can be cited before page numbers have been issued, to do this please use: T. M. W. J. Bandara, S.L.N. Senavirathna, H.M.N. Wickramasinghe, K. Vignarooban, L.A. De Silva, M. L. Dissanayake, I. Albinsson and B. Mellander, *Phys. Chem. Chem. Phys.*, 2020, DOI: 10.1039/D0CP01547D.

ROYAL SOCIETY OF CHEMISTRY

rsc.li/pccp

Binary Counter Ion Effects and Dielectric Behavior of Iodide Ion Conducting Gel-Polymer Electrolytes for High-Efficiency Quasi-Solid-State Solar Cells

T.M.W.J. Bandara[1,2], S.L.N. Senavirathna[3], H.M.N. Wickramasinghe[1], K. Vignarooban[3], L.A. De Silva[4], M.A.K.L. Dissanayake[5], I. Albinsson[6], B.-E. Mellander[2]

[1]*Department of Physics and Postgraduate Institute of Science, University of Peradeniya, Peradeniya, Sri Lanka*
[2]*Department of Physics, Chalmers University of Technology, Gothenburg, Sweden*
[3]*Department of Physics, University of Jaffna, Jaffna, Sri Lanka*
[4]*Department of Physics, University of West Georgia, Carrollton, USA*
[5]*National Institute of Fundamental Studies, Hantana Road, Kandy, Sri Lanka*
[6]*Department of Physics, University of Gothenburg, Gothenburg, Sweden*

ABSTRACT

A series of highly efficient quasi-solid-state dye-sensitized solar cells (DSCs) is prepared by harnessing the binary cation effect and positive effects of the selected performance enhancers of gel-polymer electrolytes. The new electrolyte is composed of polyacrylonitrile polymer, tetra-hexylammonium iodide (Hex_4NI) and KI binary salts as well as 4-tertbutylpyridine and 1-butyl-3-methylimidazolium iodide performance enhancers.

The charge transport in the series of electrolyte is thermally activated and, accordingly, temperature dependence of conductivity follows the VTF behavior. The enhancement of conductivity is observed with increasing mass fraction of KI and decreasing mass fraction of Hex_4NI, while the total mass fraction of salts in the electrolyte is kept unchanged. The highest conductivity of 3.74 mS cm^{-1} at ambient temperature is shown by the sample containing KI only (without Hex_4NI) at all the temperatures. The effects of dielectric polarization of the electrolytes are studied by analyzing the frequency dependence of the real and the imaginary parts of the AC conductivity in detail.

Appropriate and reproducible cell construction are assured by exhibiting efficiencies above 5% by all the quasi-solid-state DSCs assembled using double-layered TiO_2 photo-electrodes and the new electrolyte series. Besides, highlighting the mixed cation effect, the cells with mixed salts exhibited efficiencies greater than 6%. An impressively high efficiency of 7.36% was shown by the DSC prepared with electrolyte containing 75 wt.% KI and 25 wt.% Hex_4NI. This study reveals that the salt combination KI and Hex_4NI, which has not been reported before, is a suitable binary iodide salt mixture to prepare highly efficient DSCs. The replacement of tetra-hexylammonium ions by K^+ ions improves the charge transport in the electrolyte; however, the best solar cell performance is shown by the mixed salt system with 75 wt.% KI and 25 wt.% Hex_4NI, which is not the highest conductivity composition. Therefore, the exhibited high efficiency of 7.36% is evidently due to the binary cation effect.

Keywords: gel-polymer electrolytes; DSC; efficiency enhancement; counter ion; ionic conductivity; binary salt.

1. Introduction

The possibility of using gel-polymer electrolytes to enhance chemical and physical stability in dye-sensitized solar cells (DSCs) has been demonstrated since the beginning of the last two decades [1,2,3]. Recently, dye-sensitized solar cells (DSCs) based on gel-polymer electrolytes (GPEs) have gained a significant advancement over their liquid electrolyte counterparts [1,4,5,6]. It is well known that the liquid electrolytes, generally used in DSCs, ensure higher ionic conductivities and thus improves the cell efficiency, but they are still prone to chemical and physical instability [7,8]. The disadvantages of liquid electrolytes include the lack of long-term stability due to the liquid leakage, sealing difficulties,

flammability issues, corrosion of counter electrode, dye degradation, photo-degradation of constituting materials and photodecomposition of the dye in the solvent medium.

In contrast, quasi-solid-state DSCs based on GPEs have a great advantage over the aforesaid limitations. Numerous studies have been reported on finding suitable GPEs for DSCs, mainly focusing on replacing unstable liquid electrolytes by more stable gel (or quasi-solid state) polymer electrolytes [1,9]. One of the conventional ways to improve the efficiency in a DSC based on polymer electrolyte is the incorporation of plasticizers such as propylene carbonate (PC) into the electrolyte. However, since the presence of an excessive amount of solvent in the electrolyte transforms it into a viscous liquid, there is an upper limit to the solvent content to keep the electrolyte in the gel state. The present work focuses on improving DSC performance by capitalizing on the mixed counter ion effect without degrading the gel nature of the electrolyte. The work is extended to study the effects of the polarization in electrolytes by analyzing the frequency dependence of both real and imaginary parts of the AC conductivity in detail since such data is important, but lacking in the literature.

1.1. Polyacrylonitrile based GPEs

Interfacial characteristics and mechanical stability of polyacrylonitrile (PAN) based GPEs are favorable for the functioning of the devices based on gel electrolytes [10,11,12]. PAN has been successfully utilized as a host polymer matrix in Li^+ ion conducting GPEs as an electrolytic membrane for high energy density rechargeable lithium-ion batteries and photo-electrochemical solar cells [10,13,14]. DSCs prepared with PAN have exhibited higher energy conversion efficiency of about 7.27% [9,15]. Therefore, in the present work, PAN was selected as the host polymer to exploit its positive effect by the preparation of a series of quasi-solid-state electrolytes.

In PAN-based GPEs, it is generally accepted that the electrolytic solution, formed by dissolving the ionic salt in an ethylene carbonate (EC) and propylene carbonate (PC) co-solvent, is "entrapped" in cages formed by the PAN polymer matrix making the electrolyte to exhibit "liquid-like" ionic conductivity values, while maintaining a quasi-solid or gel nature [16,17]. Therefore, PAN-based gel-polymer electrolytes offer relatively higher ionic conductivities, especially at ambient temperature, and thus suitable to fabricate more stable quasi-solid-state DSCs when they are prepared with non-volatile solvents [15,17,18,19].

1.2. Iodide ion (I^-) conducting GPEs for DSCs

For the N719 dye-based DSCs, iodide ion (I^-) conductors have been established as a better choice for the redox electrolyte. One of the significant factors that influence the short circuit current density (J_{sc}) of a DSC is the iodide ion conductivity of the electrolyte. Hence, the efficiency of a solar cell is greatly dependent on the iodide ion conductivity [9,15]. The iodide ions in the electrolyte contribute to the dye regeneration process also by providing an electron to the oxidized dye. It should be noteworthy to mention that the dye plays the role of light-harvesting in DSCs, thus higher dye regeneration kinetics are necessary to achieve higher photocurrents. Therefore, faster iodide ion transport is needed to enhance dye regeneration kinetics, which in turn enhances the light-harvesting efficiency of the cell. Therefore, in order to enhance iodide ion conductivity, the iodides with bulky cations such as tetrapropylammonium iodide ($Pr_4N^+I^-$), tetrabutylammonium iodide ($Bu_4N^+I^-$) and tetrahexylammonium iodide ($Hex_4N^+I^-$) have widely been investigated [9,15,17,20]. Besides, several studies have suggested that the cation in the electrolyte has a significant positive impact on the short-circuit-current density (J_{sc}) and the electron dynamics at the electrolyte/photoelectrode interface [21,22,23]. Therefore, electrolyte cations make a major contribution to the enhancement of efficiency of DSCs.

View Article Online
DOI: 10.1039/D0CP01547D

1.3. Recent advancements

In recent literature, there are several notable innovative approaches focused on enhancing the efficiency of DSCs by improving polymer electrolytes. Very recently, Pin Ma et al. reported a novel "soggy sand" type electrolyte by integrating AlOOH nanofibers into an ionic liquid electrolyte [24]. The authors managed to increase the conductivity four times by adding AlOOH nanofibers to an ionic liquid electrolyte. Accordingly, the DSC with AlOOH nanofibers in the electrolyte has shown efficiency of 7.89%, which is a 29% increase compared to that with pure ionic liquid electrolyte [24]. In addition, the reported hybrid device prepared by amalgamation of properties of supercapacitors and DSCs gave a new insight into the research field of energy conversion and storage. Alberto Scalia et al. have designed a multipolymer electrolyte membrane separated by a cross-linked layer to combine the light-harvesting ability of DSCs and the storage ability of supercapacitors [25]. This novel hybrid photoelectrochemical device has exhibited a net conversion and storage efficiency of 3.72%, which is a remarkable value for a hybrid energy harvesting-storage device.

In another study, Federico Bella et al. reported an efficiency enhancement in aqueous electrolyte based solar cells by the treatment of $TiCl_4$ onto TiO_2 electrodes [26]. $TiCl_4$ treatment has doubled the energy conversion efficiency values and further, the study reported a higher stability over 16 days of aging the cells. The study has uncovered the importance of application of $TiCl_4$ treatment even for liquid electrolytes based DSCs [26]. Another important study reports an investigation on nanoscale growth and crosslinking of a polymer electrolyte inside the nanostructured photoelectrode. In the study, [27] the electrochemical and photovoltaic performance dependence on thickness and degree of penetration of the electrolyte has been investigated and thus, managed to optimize the amount

of polymer, cell efficiency and stability. Importantly, the cell stability test conducted for 1000 h proved the higher stability offered by polymer electrolytes [27].

Very recently, Liu et al. [28] reported another new approach by introducing carbon nanotube (CNT) electrolytes intended for DSCs. The role of CNT in the electrolyte deviates from the role of conventional gelators. However, the authors managed to improve the efficiency from 8.15% to 8.70% as a result of the improvement of open-circuit voltage by added CNT [28].

Binary-counter ion effect

As reported recently, GPEs with a mixture or a combination of iodide salts have shown improvement of DSC performance compared to that of single salt electrolytes [18,19,29,30,31,32]. The effect has been attributed to the dual role played by small and large cations to stimulate the photo-current and photo-voltage. The method provides a way to improve DSC performance without degrading the mechanical properties of the electrolyte.

The bulky cations such as Pr_4N^+, Bu_4N^+ and Hex_4N^+ are known to minimize the cationic conductivity and, in turn, improve the iodide ion conductivity in the electrolyte. Cations with high charge density, such as Li^+, Na^+ or K^+, get absorbed into the TiO_2 electrode and consequently lead to improved photogeneration of electrons in the dye and improved diffusion dynamics at the dye-semiconductor interface [18,19,24].

In order to make use of both aforesaid mechanisms, it would be better to explore the combined effect of binary mixtures of iodide salts (one with a bulky cation and the other with a small alkali cation) in electrolytes. To investigate these binary cation effects in detail, we have studied the present system by choosing KI as the salt with small alkali and Hex_4NI as the salt with a bulky quarteneryammonium cation. This study aims at enhancing the efficiency of DSCs composed of PAN-based GPEs. For this purpose, the composition of

View Article Online
DOI: 10.1039/D0CP01547D

binary mixture of iodides KI and Hex_4NI is optimized in order to maximize the short circuit photocurrent density through enhanced iodide ion conductivity. To our knowledge, only a few studies are reported in the literature on utilizing this type of binary iodide salt mixture on the efficiency enhancement in quasi-solid-state DSCs, and this is the first report on GPEs made with KI and Hex_4NI mixed iodide salt system intended to enhance efficiency in DSCs. In this work 4-tertbutylpyridine (4TBP) and 1-butyl-3-methylimidazolium iodide (BMII) have been used as additives to get better DSC performance [33] and hence to get impressively higher DSC performance.

2. Experimental

2.1 Preparation of electrolyte

Polyacrylonitrile (PAN), tetrahexylammonium iodide, KI, iodine (I_2), PC and EC (all with purity greater than 98%) purchased from Sigma-Aldrich were used as starting materials. PAN, KI, and Hex_4NI were vacuum dried at 60 °C for 24 h prior to use. Weights of EC (1.6604 g), PC (1.5404 g), 4TBP (0.0868 g) and BMII (0.0504 g) were kept unchanged in all the electrolyte samples. The relative weights of KI and Hex_4NI were varied, keeping their total weight constant at 0.37 g. The weight of iodine (I_2) was 0.384 g, which is about one-tenth of the total mole amount of the iodide from the two salts. Appropriately weighed quantities of EC, PC, 4TBP, BMII, KI and Hex_4NI were mixed under the continuous stirring at room temperature for ~2 h until the entire amount of salts dissolves. Then, after adding 0.4 g of PAN, the mixture was stirred again for about 30 min. Then the mixture was heated to about 80 °C together with continued stirring for about another 15 min. The resulting mixture was allowed to cool down to ambient temperature. Finally, I_2 chips (384 mg) were added and again continuously stirred overnight in a closed bottle to obtain a homogeneous gel-electrolyte. This procedure was repeated for all the electrolyte compositions given in Table 1.

Three electrolytes samples were prepared and tested for each composition and the samples with most reproducible results were selected for the analysis.

Table 1: Weights and weight fractions (percentages) of KI and Hex_4NI used to prepare the PAN-based gel-polymer electrolytes.

Electrolyte	KI wt.%	Hex_4NI wt.%	KI / mg	Hex_4NI / mg
A	0	100	0	370.0
B	25	75	92.7	277.5
C	50	50	185.0	185.0
D	75	25	277.5	92.7
E	100	0	370.0	0.0

2.2 Electrolyte characterization

Ionic conductivities of the five electrolyte samples were extracted from the complex impedance spectroscopic data measured using Metrohm Autolab (PGSTAT 128N, Netherlands) impedance analyzer in the frequency range 1 Hz–1 MHz. For this purpose, the electrolytes were sandwiched between two polished stainless steel (SS) electrodes with configuration SS/electrolyte/SS. The temperature of the electrolyte sample was varied from ~75 °C to room temperature at ~5 °C steps. The temperature of the sample was allowed to stabilize for ~15 min for each measurement. The measurements were taken on the cooling runs (from 75 °C to 23 °C). The bulk DC conductivity and complex AC conductivity values of the electrolytes were calculated from the impedance data. The glass transition temperatures of the electrolytes were estimated by using a Mettler Toledo DSC 30 differential scanning calorimeter. The temperature scanning was conducted between −120 °C and 120 under ±10 °C min^{-1} heating/cooling rate.

View Article Online
DOI: 10.1039/D0CP01547D

2.3 TiO_2 electrode preparation

Two successive layers of TiO_2 were deposited on the FTO conducting glass substrate in order to prepare the photo-anode. The mixture for the 1st layer was prepared by grinding 0.5 g of P90, TiO_2 nanoparticles (Evonik-Degussa) with 2 ml of 0.1 M nitric acid, in a mortar for ~30 min. The resulting slurry was coated on a well-cleaned FTO glass substrate by spinning at a speed of 2,300 RPM for 60 s. During the spin-coating, a part of the glass plate was covered with an adhesive tape to prevent coating TiO_2 on the area needed for electrical contacts. After air-drying for 30 min, the TiO_2 coated electrodes were sintered at 450 °C for ~30 min and subsequently allowed to cool down gradually to room temperature (-0.5 °C/min). Subsequently, the second layer of TiO_2 was coated on the top of the first layer using P25 TiO_2 nanoparticles (Evonik-Degussa). For the preparation of this layer, 0.5 g of TiO_2 powder was ground well for ~30 min with 2 ml of 0.1 M nitric acid in a mortar. Subsequently, 0.1 g of Carbowax and a few drops of Triton X 100 (surfactant) were added and continued the mixing for another few min. This colloidal suspension was cast using the doctor blade method followed by sintering at 450 °C for 30 min to obtain a porous layer of TiO_2 nanoparticles. Finally, the dye sensitization process was carried out by immersing the TiO_2 coated glass plates in a saturated solution of ruthenium N719 (Solaronix SA) in ethanol. The temperature of the dye solution is 60 °C at the dipping, and then kept soaked in for ~24 h at the room temperature.

2.4 Solar cell fabrication and characterization

Gel-polymer electrolyte-based DSCs, with the configuration FTO/TiO_2/dye/electrolyte/Pt/FTO were assembled by sandwiching the electrolyte film between the dye-sensitized TiO_2 electrode and the Pt counter electrode (Pt-coated glass). The photo-current voltage (*I-V*) characteristics of the solar cells were measured under the

irradiation of 1000 W m^{-2} (1.5 AM) with a solar simulator (ABET technologies) using a 0.19 mm^2 aperture. Current-voltage data were measured and recorded using a Metrohm Autolab (PGSTAT 128N) with Nova software at the scan rate of 0.1 V s^{-1}. Three cells of each composition were tested and the most stable was selected for the analysis.

3. Results and Discussion

3.1 DC conductivity

The temperature dependence of ionic conductivity of the electrolytes is illustrated in Fig. 1. In order to calculate these ionic conductivities, the bulk DC resistances of the electrolytes were extracted from Nyquist plots. As an example, the Nyquist plots of sample *A* taken at different temperatures between 23 °C and 70 °C are shown in Fig. 2. All the other samples (*B* to *E*) also exhibited similar curves (not shown). The DC resistance values obtained were used to estimate the ionic conductivity of the electrolytes shown in Fig. 1.

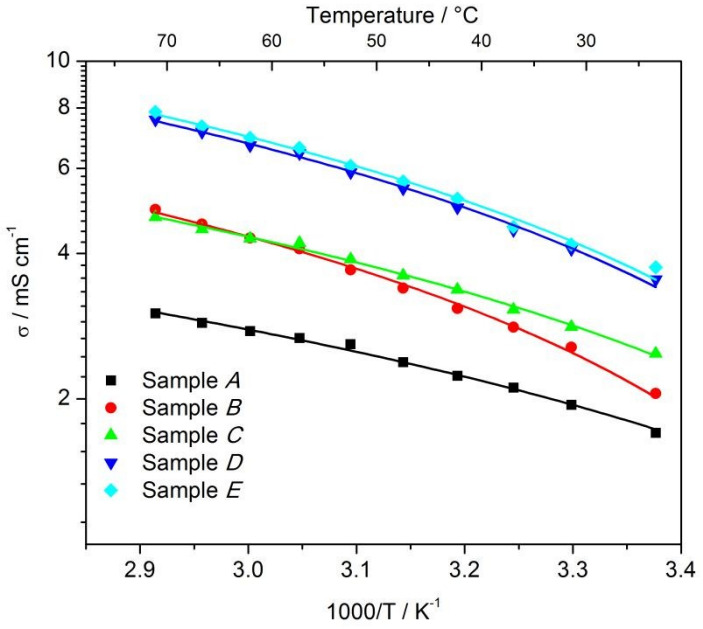

Fig. 1: Conductivity Arrhenius plots of the PAN-based GPEs prepared with different amounts of KI and Hex_4NI salts.

View Article Online
DOI: 10.1039/D0CP01547D

The trend seen in Fig. 1 is non-Arrhenius. The ionic conductivity of this gel electrolyte increases with the increased amount of KI and the decreased amount of Hex_4NI. This behavior is expected since the contribution to the conductivity from ionic mobility of the bulky cation Hex^+ is very small compared to that of small size cation K^+, as inferred from transference number studies given for the analogous systems [30, 31]. As shown in Fig. 1, the highest conductivity is exhibited by the electrolyte, which has 100% KI and 0% Hex_4NI mass fractions (sample *E*). The room temperature conductivity of this electrolyte sample, *E*, is as high as 3.74 mS cm^{-1}. The conductivities of this sample at 50 and 70 °C are 6.07 and 7.86 mS cm^{-1} respectively. It is also seen that the conductivities of the electrolyte samples *D* and *E,* in the studied temperature range, are close to each other. The recorded conductivities of all the electrolytes are sufficiently high enough to prepare high-efficiency quasi-solid-state DSCs. However, it should be noted that the ionic conductivities of all these electrolyte samples consist of contributions from both cations and anions. Samples *D* and *E* exhibit higher ionic conductivities than that of other samples, evidently due to the contribution of higher concentration of small-sized K^+ ions with higher mobility in these samples. However, it will be the contribution from iodide anions (I^-) which would eventually determine the short circuit photocurrent density as already reported for several DSC systems [18,19, 30]. Due to this factor, the electrolytes that give higher iodide ion conductivity are more suitable to fabricate highly efficient DSCs. In this context, previous studies have demonstrated in detail the advantages of using a combination of iodide salts containing small and large cations instead of a single iodide salt electrolytes in order to enhance the performance of quasi-solid-state DSCs [19, 30].

View Article Online
DOI: 10.1039/D0CP01547D

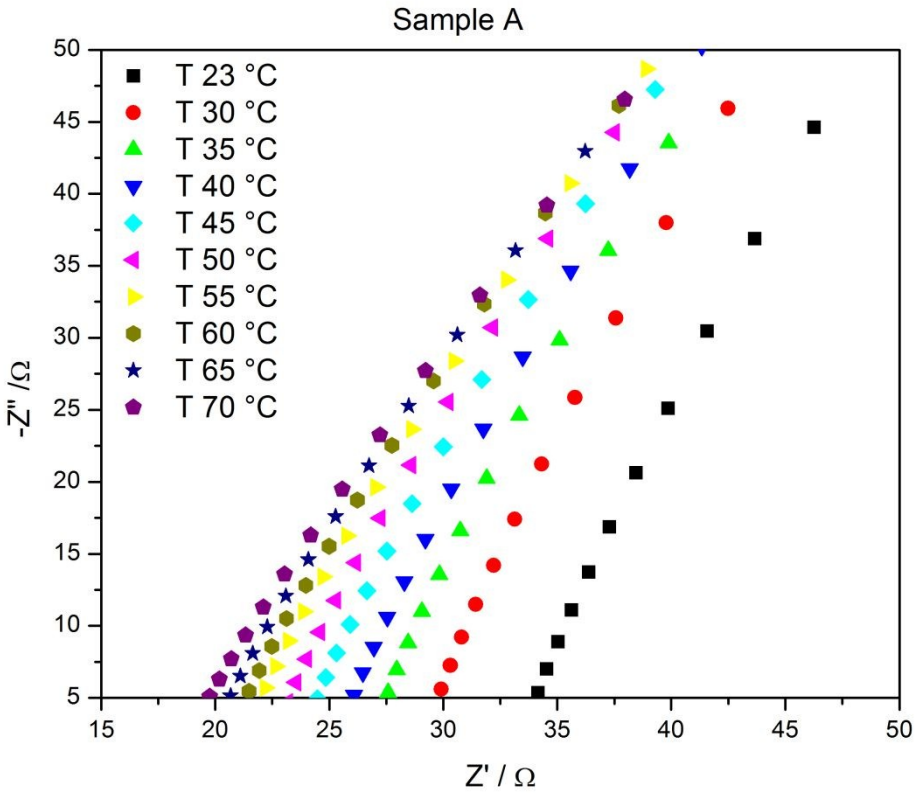

Fig. 2: Nyquist plots for electrolyte sample *A* (containing 100% Hex_4NI) taken at different temperatures from 23 to 70 °C.

Since Fig. 1 is non-Arrhenius, $\ln(\sigma T^{1/2})$ is plotted as a function of $(T\text{-}T_g)$ (in Fig. 3) in order to understand the temperature dependence of the conductivity. As clearly shown in Fig. 3, the conductivity variation with temperature exhibits VTF (Vogel-Tammann-Fulcher) type behavior [34,35]. The measured glass transition temperatures (T_g) of the samples are about 100 °C. These measured glass transition temperatures were used at T_0 for the curve fitting. The appropriateness of this selection of T_g as T_0 is confirmed by the better fitting shown in Fig. 3. The pseudo activation energy and pre-exponential factors were calculated by fitting the data to the VTF equation (1) and tabulated in Table 2.

View Article Online
DOI: 10.1039/D0CP01547D

$$\sigma(T) = AT^{-1/2} \exp\left[-E_a / k_B(T - T_0)\right] \quad (1)$$

The activation energy (E_a) and pre-exponential factor (A) increase with increasing mass fraction of KI except for sample B. Sample B has shown slightly lower activation energy, which can be attributed to higher disorder imposed by the addition of small amounts of KI to the single salt system. Added disorder can improve the amorphousity of the electrolyte leading to enhancement of the ionic conductivity [35].

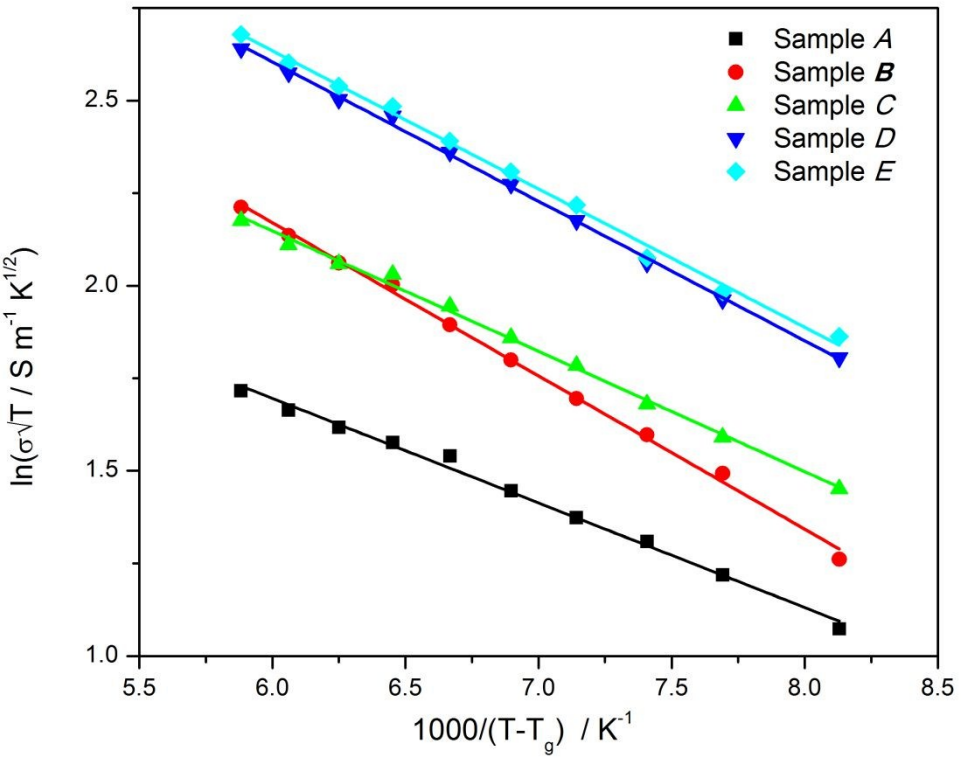

Fig. 3: ln($\sigma T^{1/2}$) versus (T-T_g) plots of the PAN-based GPEs prepared with different amounts of KI and Hex_4NI salts.

View Article Online
DOI: 10.1039/D0CP01547D

Table 2: The activation energy, E_a, and pre-exponential factor, A, for electrolytes with different mass fractions of KI and Hex_4NI salts given in Table 1.

Sample	A / S m^{-1} K$^{1/2}$	E_a / eV
A	29.67	0.024
B	104.97	0.035
C	60.22	0.028
D	129.49	0.032
E	130.96	0.032

3.2 Complex AC conductivity

In general, the complex conductivity in an electrolyte is affected by different types of polarization [36]. The electrolytes studied in this work can undergo different polarizations such as electrode polarization, dipole polarization, ionic polarization, as well as electronic polarization due to their complex nature. Besides, dielectric relaxations and the dynamics of ionic species and dipoles can modify the ionic conduction as well as the dielectric behavior of the electrolyte. Therefore, the real and the imaginary parts of the AC conductivity of electrolytes are investigated as a function of frequency at different temperatures.

Variations of the real part of the AC conductivities ($\sigma'_{(\omega)}$) of the series of electrolytes (from *A*-*E*) are shown in Fig. 4, as a function of the frequency at different temperatures. Apparently, all the AC conductivity curves reach plateau values at low frequencies as well as at high frequencies. The high-frequency plateaus in Fig. 4 can be attributed to reaching the conductivity to its DC limit. These high-frequency values are comparable with the DC conductivities calculated using Nyquist plots. In order to analyze and compare these high-frequency plateau values of AC conductivity (σ') with the DC conductivity, the values at 10^5 Hz are given in Table 3. These high-frequency plateau values increase with increasing

temperature for all the samples, which can lead to increased ion transport kinetics with increasing temperature. They are comparable with the conductivities given in Fig. 1.

As seen from Figs. 4 (A)-(E), with decreasing frequency, the AC conductivity drops exponentially, and the trend can be attributed to the limitations in change of polarization with frequency. Therefore, a strong frequency and temperature dependence of $\sigma'_{(\omega)}$ can be observed in all the samples. In order to understand the exponential drop of σ' at low frequencies ($1Hz \leq f \leq 100\ Hz$), σ' is plotted in logarithmic scale and shown in the insets of Figs. 4 (A)-(E). Though it appears that σ' reaches a plateau at low frequencies, the actual trend at low frequency is an exponential drop with decreasing frequencies as seen from the insets of Figs. 4 (A)-(E). This exponential drop can be related to electrode polarization effects [37,38], which in general increases with decreasing frequency. Simply at low frequencies, more charges accumulate at the electrode-electrolyte interface resulting in a decrease in the number of mobile ions in the bulk. This reduction of charge carrier concentration in the bulk reduces the conductivity, as seen in Fig. 4. However, owing to the fast charge transport dynamics of this electrolyte, the high-frequency dispersive part is not visible in the measured frequency range [37, 38]. In order to understand the polarization effects governed by ionic motion in the bulk, the low-frequency part of the $\sigma'_{(\omega)}$ is fitted to the equation:

$$\sigma'_{(\omega)} = A\omega^n \qquad (2)$$

where ω is the angular frequency of the applied AC signal and n is a factor which depends on the polarization. The parameter n is calculated for all the samples and tabulated in Table 4, which can possibly be used as a measure of interfacial polarization.

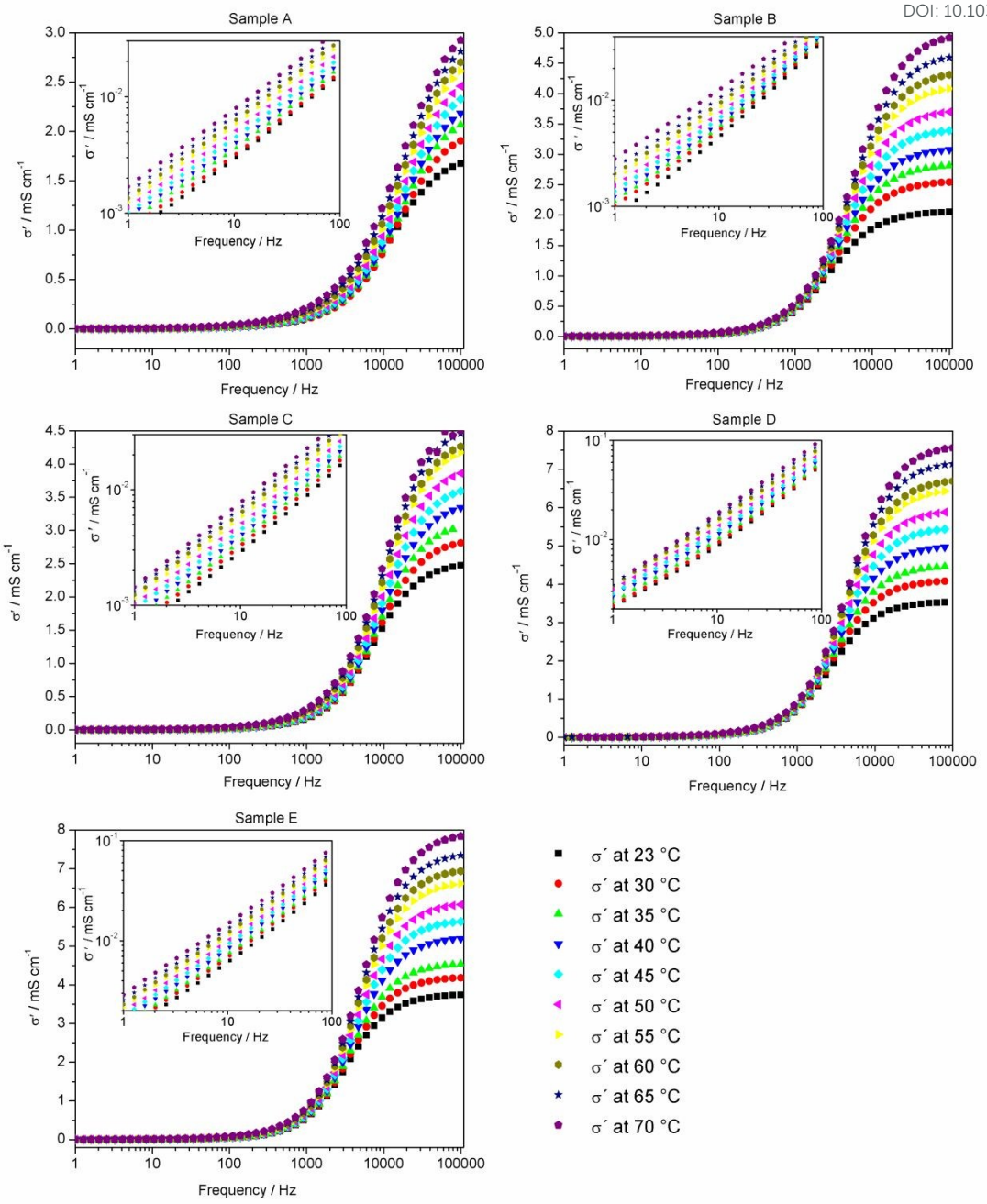

Fig. 4: Frequency dependence of real part of the AC conductivity ($\sigma'_{(\omega)}$) in electrolyte samples, with different amounts of KI and Hex_4NI, at different temperatures. The inset of each curve shows the low-frequency part of $\sigma'_{(\omega)}$.

View Article Online
DOI: 10.1039/D0CP01547D

Table 3: AC conductivity ($\sigma'_{(\omega)}$) values at 10^5 Hz in mS cm^{-1} for the electrolytes given in Table 1 at different temperatures.

Sample	23 / °C	30 / °C	40 / °C	50 / °C	60 / °C	70 / °C
A	1.68	1.91	2.18	2.46	2.70	2.93
B	2.05	2.54	3.08	3.70	4.31	4.92
C	2.47	2.81	3.34	3.65	4.26	4.50
D	3.53	4.08	4.97	5.88	6.69	7.56
E	3.74	4.18	5.19	6.07	6.94	7.84

Table 4: *n* values in equation (2) for the electrolytes given in Table 1 at different temperatures.

Sample	23 / °C	30 / °C	40 / °C	50 / °C	60 / °C	70 / °C
A	0.75	0.75	0.73	0.72	0.71	0.70
B	0.78	0.79	0.79	0.78	0.76	0.74
C	0.82	0.82	0.81	0.80	0.79	0.77
D	0.78	0.79	0.78	0.78	0.76	0.76
E	0.81	0.81	0.81	0.81	0.80	0.78

The imaginary part of the complex conductivity ($\sigma''_{(\omega)}$) is also plotted against frequency for each sample at different temperatures and shown in Fig. 5. All the curves show a similar trend, but move upward with increasing temperature. In general, the imaginary part, σ'', is resulted by the contribution of capacitive effects of the cell prepared by sandwiching an electrolyte between two SS blocking electrodes. The imaginary part of the complex conductivity peak values seen at about 10 kHz can be due to the relaxation of interfacial charge transport which more or less increases with increasing mass fraction of KI. The temperature dependence of the peak values of σ'' is also shown in Fig. 5. The exhibited

relatively larger peaks by sample B at higher temperatures (Fig. 5), this may be a consequence of lower conductivity activation energy (Table 2) of the sample.

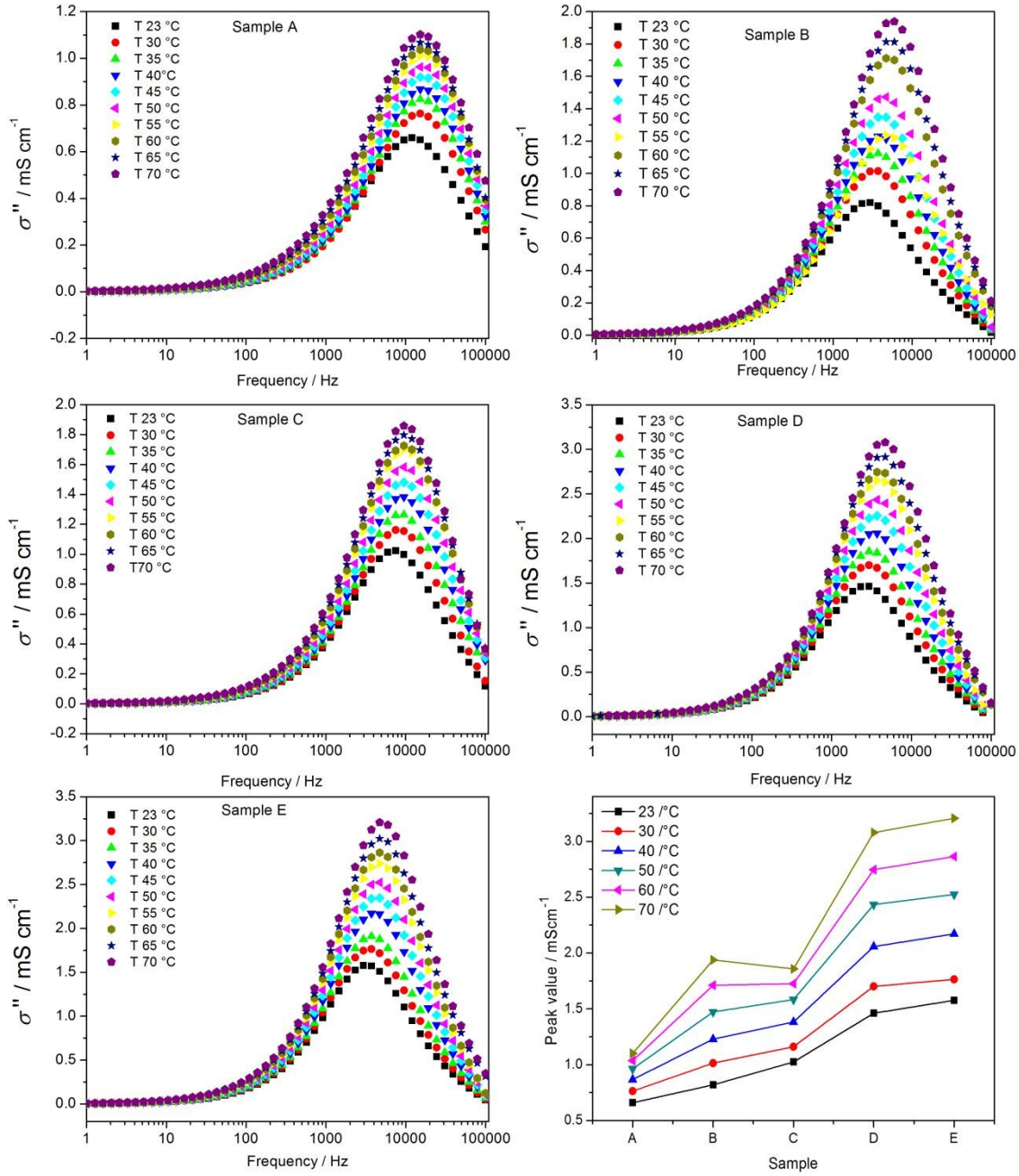

Fig. 5: The imaginary part of the AC conductivity (σ'') isotherms of electrolyte samples as a function of frequency. The bottom curve at the right shows the peak values of σ'' of the samples at different temperatures.

The tangent of the phase angle ($\tan\phi = -\frac{Z''}{Z'}$) of the impedance is also plotted against the frequency for each sample at various temperatures and shown in Figs. 6 (A-E). The peak values of $\tan\phi$ are also shown in Fig. 6. These relaxation times (time constant) correspond to peak values, which are related to electrode polarization. The peak height is increasing with the increasing mass fraction of KI except for sample B. Relatively higher peak values shown by sample B can be attributed to the lower conductivity activation energy. As seen in Fig. 6, time constant related to electrode polarization is decreasing with increasing temperature as a result of faster charge transport dynamics at higher temperatures.

View Article Online
DOI: 10.1039/D0CP01547D

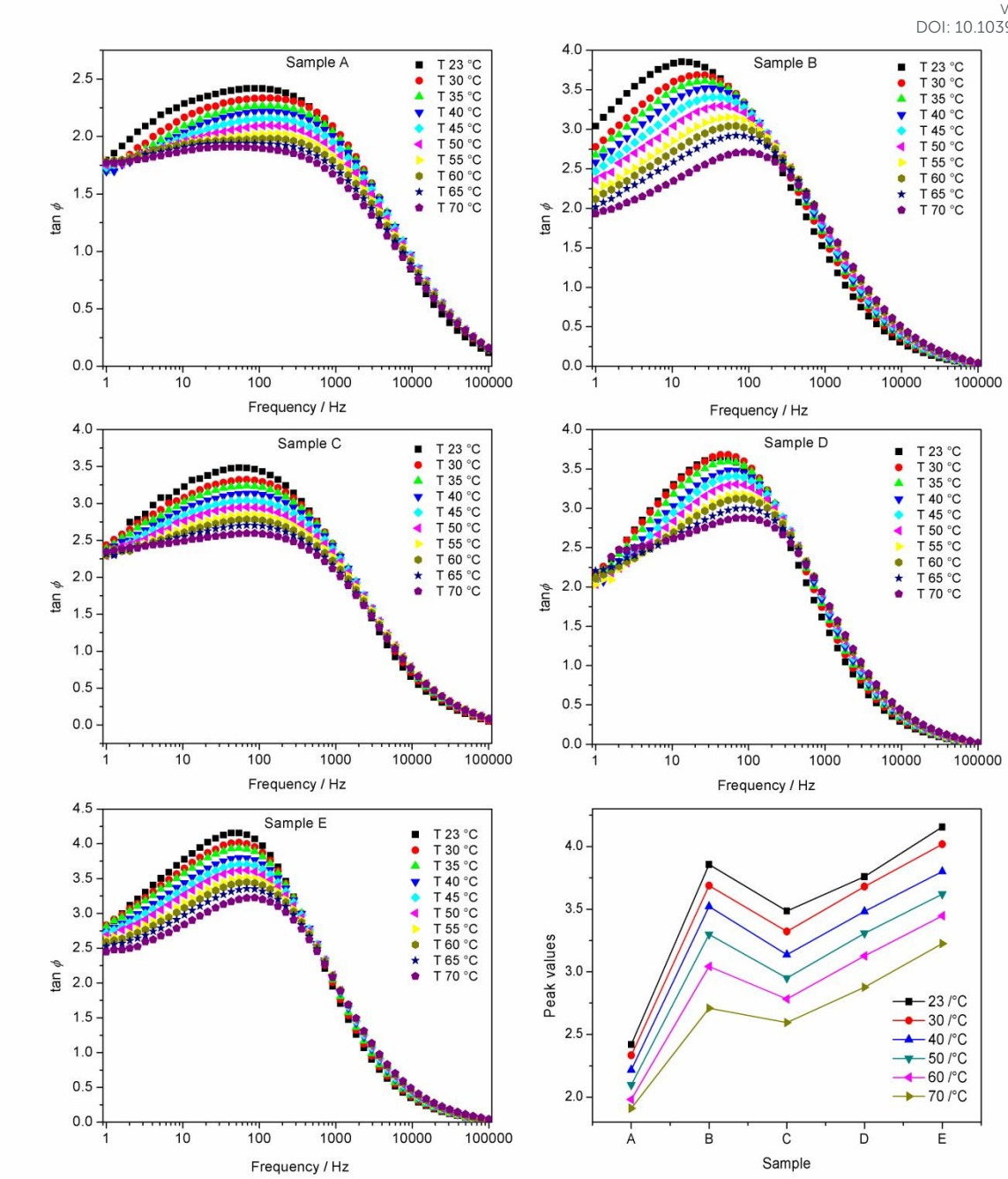

Fig. 6: The tangent of the phase angle $(\tan\phi = -\frac{Z''}{Z'})$ of the impedance against the frequency for electrolyte samples at various temperatures. The bottom curve at the right shows the peak values of the samples at different temperatures.

3.3 DSC characterization

The influence of cations (couterions) on the performance of gel polymer electrolytes based DSCs can be investigated by separating their contribution into two categories. 1) the effect of the nature of cations in the electrolyte to modify the conductivity in the electrolyte. 2) cations in the electrolyte, depending on their size and charge density, get adsorbed onto or intercalate into the nanostructured TiO_2 electrode and modify the conduction band edge of the TiO_2 film [22,30,39].

The 1st effect can be understood by studying the ionic conductivity of the electrolyte as we did this work by analyzing AC and DC conductivities. The charge transport process of a DSC is governed by the conductivity in the electrolyte since the series resistance of a functioning DSC is dominantly contributed by the resistance of the electrolyte. Therefore, as generally accepted, the photocurrent and the short circuit current density of a DSC are governed by the conductivity in the electrolyte, or in particular, by I^-/I^{-3} conductivity. The conductivity in polymer electrolytes (as shown in Figure 1), drastically depends on the nature of the cation as described in detail [22], due to ion polymer interactions do change the chemical and physical surrounding of mobile ionic species. The 2nd effect can be understood by studying the shift of conduction band edge as well as influence to alter the Helmholtz double layer at the electrolyte photoelectrode interface, as explained in detail [30,40,41]. Mainly, the V_{oc} of the cell governed by this effect [39]. When the cell is at the open circuit, the electrical current does not flow through the external circuit, and the V_{oc} is the shift of Fermi level of the photoelectrode relative to the redox level of the electrolyte, at the equilibrium. The shift of the Fermi level is controlled by the number of photo-generated electrons in the conduction band of a functioning cell, at the equilibrium [22]. High charge density cations, such as Li^+, in the electrolyte, get adsorbed in to the TiO_2 structure and make a positive shift of the conduction band, thereby facilitating the photoelectron

generation and enhancing the photocurrent. This is also associated with a drop in the Voc. As it hinders the relative shit of the conduction band as well as the Fermi level resulting in a drop of V_{oc}.

A series of DSCs were assembled using KI and Hex_4NI based electrolyte samples prepared according to the compositions given in Table 1. Photocurrent density and power density versus cell potential (*J-V*) curves were used to calculate the short circuit current density (J_{sc}), the open-circuit voltage (V_{oc}) and the energy conversion efficiency. The variation of V_{oc}, J_{sc} and the energy conversion efficiency of the electrolytes with the increasing amount of KI and decreasing amount of Hex_4NI are shown in Figs. 7 and 8.

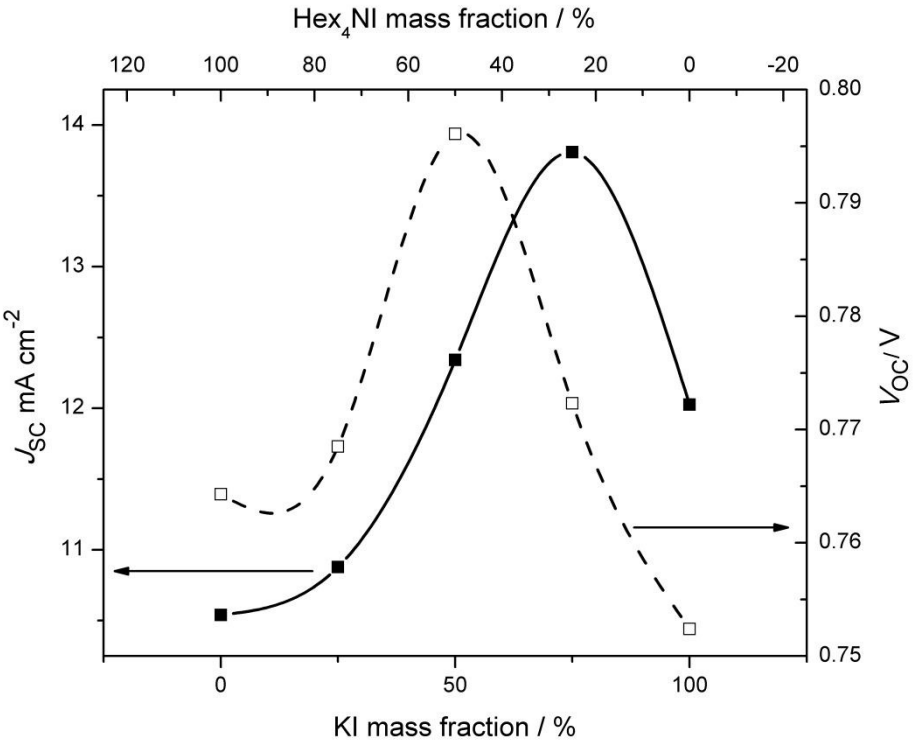

Fig. 7: Variation of V_{oc} and J_{sc} in DSCs as a function of KI and Hex_4NI contents in the electrolyte.

The present work also clearly demonstrates the mixed cation effect on the performance of DSCs based on GPEs [18,19, 24]. The ionic conductivity of this electrolyte increases with

View Article Online
DOI: 10.1039/D0CP01547D

the increasing amount of the KI and decreasing amount of the Hex_4NI, as shown in Fig. 1. However, as seen in Figs. 7 and 8, the solar cell parameters do not follow the trend of ionic conductivity. According to Fig. 7, the highest V_{oc} is given by the cell containing electrolyte sample *C* with 50% KI and 50% Hex_4NI. Higher V_{oc} values are expected from the electrolytes with larger cations [22,31], and accordingly the cell with electrolyte sample *A* should exhibit the highest V_{oc}. Conversely, the ionic conductivity, which also is essential for the higher performance of a DSC, decreases with the increasing amount of lager cationic salt Hex_4NI. As a result of above mentioned two competing effects, the highest V_{oc} of 796 mV is exhibited by the cell containing electrolyte sample *C*.

The photocurrent density of a DSC depends on the ionic conductivity of the electrolyte, in particular, the iodide ion conductivity. In addition, the iodide ion conductivity drives the charge injection at the photoelectrode/electrolyte interface by improving the regeneration kinetics of the dye sensitizer. Further, the cations in the electrolyte can govern the flat-band potentials of TiO_2 due to intercalation and adsorption of cations to the photo-electrode. In general, J_{sc} in this type of DSC depends primarily on the anionic conductivity in the electrolyte. The highest J_{sc}, as shown in Fig. 8, is given by the cell with electrolyte sample *D,* which contains KI (75 wt.%) and Hex_4NI (25 wt.%). Though single salt system (sample *E* with 100 wt.% KI) exhibits the highest ionic conductivity than that of sample *D* (mixed salt system), the mixed cation effect has contributed to give the highest J_{sc} for the cell with electrolyte *D*. Moreover, in sample *E*, a significant contribution to the total ionic conductivity comes from the K^+ ion conductivity as well, which does not directly contribute to J_{sc}. The incorporation of 25 wt.% of Hex_4NI (a salt with lager cation) can shift flat band potentials to more towards the negative potential and thus can increase the charge injection

rates contributing to J_{sc} enhancement. As a result, the highest J_{sc} of 13.8 mA cm^{-2} is shown by the DSC with electrolyte sample D.

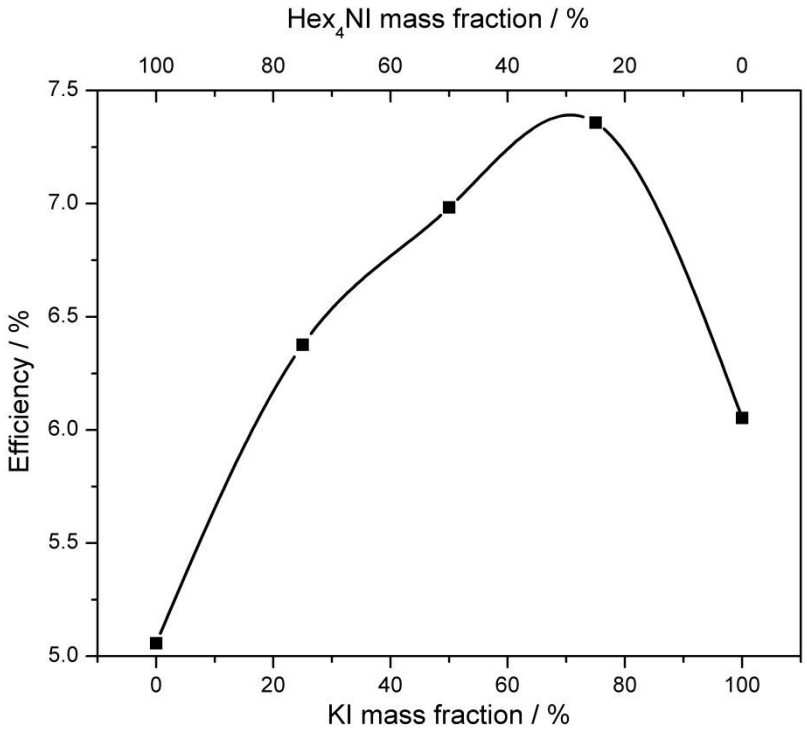

Fig. 8: Variation of the energy conversion efficiency in DSCs as a function of KI and Hex_4NI composition ratio in the electrolyte.

The energy conversion efficiencies of the DSCs prepared are shown in Fig. 8. All the cells studied in this work have shown efficiencies over 5%. Each and every cell prepared in this study (including three cells prepared with each composition) exhibited efficiencies above 5% and the photocurrent did not show any sign of a degradation within the continued irradiation of about one hour. Highlighting the mixed salt effect, the cells with mixed salts have shown efficiencies greater than 6%. Consequently, an impressively high efficiency of 7.36% is shown by the quasi-solid-state DSC prepared with electrolyte sample D. This study

View Article Online
DOI: 10.1039/D0CP01547D

suggests that the salt combination KI and Hex_4NI is a novel iodide salt mixture suitable to fabricate highly efficient DSCs. Further, since we did not include any volatile solvents, such as acetonitrile, acetone, ethanol, etc. in the electrolyte, the fabricated DSC is an environmentally friendly, stable device with a significantly high energy conversion efficiency of 7.36%.

4. Conclusions

A new set of GPEs based on the PAN polymer host, which is suitable to fabricate highly efficient quasi-solid-state DSCs harnessing the mixed cation effect, were investigated. The new GPEs are composed of PC and EC co-solvents, tetrahexylammonium iodide (Hex_4NI) and KI salts and 4-tertbutylpyridine and 1-butyl-3-methylimidazolium iodide performance enhancers. The analysis of ionic conductivity in electrolytes reveals that the temperature dependence of the electrolyte exhibits VTF (non-Arrhenius) behavior. The ionic conductivity in the electrolyte increases with the increasing mass fraction of KI (decrease of Hex_4NI). The highest conductivities at all the temperatures are given for sample *E* with 100 wt.% KI and it shows values of 3.74, 6.07 and 7.86 mS cm^{-1} at 23, 50 and 70 °C, respectively. Frequency dependence of the real and imaginary parts of the AC conductivity is analyzed in order to understand polarization effects on electrical/dielectric properties. The real part of the AC conductivity increases with increasing temperature as well as increasing frequency as a result of an increase in ion transport dynamics. Peak values of the imaginary part of the AC conductivity are visible at about 10 kHz due to charge transport relaxation.

A set of DSCs assembled using N719 dye-sensitized TiO_2 electrodes and the new electrolyte series showed efficiencies higher than 5%. Highlighting the mixed cation effect, the cells with mixed iodide salts show efficiencies greater than 6%. Consequently, an impressively

high energy conversion efficiency of 7.36% is achieved by the quasi-solid-state DSC prepared with electrolyte containing 75% KI and 25% Hex_4NI. This study suggests that the salt combination KI and Hex_4NI provides a suitable iodide salt mixture for the fabrication of high-efficiency DSCs.

Acknowledgment

Research support from the University of Peradeniya Sri Lanka, University Research Grant No. URG/2019/27IS, is gratefully acknowledged.

References

[1] F. Bella, Polymer electrolytes and perovskites: lights and shadows in photovoltaic devices, Electrochimica Acta. 175 (2015) 151-161.

[2] M. A. K. L. Dissanayake, L. R. A. K. Bandara, R. S. P. Bokalawala, P. A. R. D. Jayathilaka, O. A. Ileperuma, S. Somasundaram, A novel gel polymer electrolyte based on polyacrylonitrile (PAN) and its application in a solar cell, Materials Research Bulletin. 37 (2002) 867-874.

[3] O. A. Ileperuma, M. A. K. L. Dissanayake, S. Somasundaram, Dye-sensitised photoelectrochemical solar cells with polyacrylonitrile based solid polymer electrolytes, Electrochimica Acta. 47 (2002) 2801-2807.

[4] Umer Mehmood, Saleem-ur Rahman, Khalil Harrabi, Ibnelwaleed A. Hussein, B. V. S. Reddy, Recent advances in dye sensitized solar cells, Advances in Materials Science and Engineering (2014). http://dx.doi.org/10.1155/2014/974782.

[5] Lei Fan, Shuya Wei, Siyuan Li, Qi Li, Yingying Lu, Recent progress of the solid-state electrolytes for high-energy metal-based batteries, Advanced Energy Materials. 8 (2018) 1702657.

[6] S. J. Lue, Yun-Ling Wu, Yung-Liang Tung, Chao-Ming Shih, Yi-Chun Wang, Jun-Ruei Li, Functional titanium oxide nano-particles as electron lifetime, electrical conductance enhancer, and long-term performance booster in quasi-solid-state

View Article Online
DOI: 10.1039/D0CP01547D

electrolyte for dye-sensitized solar cells. Journal of Power Sources 274 (2015) 1283-1291.

[7] D.S. Huo Z, Kongjia Wang, Fantai Kong, Changneng Zhang, Xu Pan, Xiaqin Fang, Nanocomposite gel electrolyte with large enhanced charge transport properties of an I3/I redox couple for quasi-solid-state dye sensitized solar cells, Sol Energy Mater Sol Cell. 91 (2007) 1959–1965.

[8] Kun-Mu Lee, Vembu Suryanarayanan, Kuo-Chuan Ho, Influences of different TiO_2 morphologies and solvents on the photovoltaic performance of dye-sensitized solar cells, J Power Sources 188, (2009) 635–641.

[9] O. A. Ileperuma, Gel polymer electrolytes for dye sensitized solar cells: a review, Materials Technology. 28 (2013) 65-70.

[10] M. S. Su'ait, Mohd Yusri Abd Rahman, Azizan Ahmad, Review on polymer electrolyte in dye-sensitized solar cells (DSCs), Solar Energy. 115 (2015) 452-470..

[11] K. S. Ngai, S. Ramesh, K. Ramesh, J. C. Juan, A review of polymer electrolytes: fundamental, approaches and application, Ionics. 22 (2016) 1259-1279.

[12] O. A. Ileperuma, K. Murakami, Quasi-solid polymer electrolytes based on polyacrylonitrile and plasticizers for indoline dye sensitized solar cells of efficiency 5.3 %, Chem Lett. 37 (2008) 36.

[13] K. M. Abraham, Li^+ -conductive solid polymer electrolytes with liquid-like conductivity, J Electrochem Soc. 137 (1990) 1657.

[14] G. Dautzenberg, S. Passerini, B. Scrosati, Characterization of PAN-based gel electrolytes. Electrochemical stability and lithium cyclability, Chem Mater. 6 (1994) 538.

[15] O. A. Ileperuma, G. R. Asoka Kumara, Hong-Sheng Yang, Kenji Murakami, Quasi-solid electrolyte based on polyacrylonitrile for dye-sensitized solar cells, Journal of Photochemistry and Photobiology A: Chemistry 217 (2011) 308-312.

[16] S. AM, Review on gel polymer electrolytes for lithium batteries, Eur Polymer J. 42 (2006) 21.

View Article Online
DOI: 10.1039/D0CP01547D

[17] O. A. Ileperuma, K. Murakami, Quasi-solid polymer electrolytes based on polyacrylonitrile and plasticizers for indoline dye sensitized solar cells of efficiency 5.3 %, Chem Lett. 37 (2008) 36.

[18] T. M. W. J. Bandara, M. F. Aziz, H. D. N. S. Fernando, M. A. Careem, A. K. Arof, B. E. Mellander, Efficiency enhancement in dye-sensitized solar cells with a novel PAN-based gel polymer electrolyte with ternary iodides, Journal of Solid State Electrochemistry. 19 (2015) 2353-2359.

[19] T. M. W. J. Bandara, H. D. N. S. Fernando, M. Furlani, I. Albinsson, J. L. Ratnasekera, L. A. DeSilva, B. E. Mellander, Combined effect of alkaline cations and organic additives for iodide ion conducting gel polymer electrolytes to enhance efficiency in dye sensitized solar cells, Electrochimica Acta. 252 (2017) 208-214.

[20] T. M. W. J. Bandara, T. Svensson, M. A. K. L. Dissanayake, M. Furlani, W. J. M. J. S. R. Jayasundara, and B-E. Mellander, Tetrahexylammonium iodide containing solid and gel polymer electrolytes for dye sensitized solar cells, Energy Procedia 14 (2012) 1607-1612.

[21] S. Kambe, S. Nakade T. Kitamura, Y. Wada, S. Yanagida, Influence of the electrolytes on electron transport in mesoporous TiO_2-elecetrolyte system, The Journal of Physical Chemistry B. 106 (2002) 2967-2972.

[22] T. M. W. J. Bandara, H. D. N. S. Fernando, M. Furlani, I. Albinsson, M. A. K. L. Dissanayake, J. L. Ratnasekera, B-E. Mellander, Effect of the alkaline cation size on the conductivity in gel polymer electrolytes and their influence on photo electrochemical solar cells, Physical Chemistry Chemical Physics. 18 (2016) 10873-10881.

[23] X. Shen, Weilin Xu, Jie Xu, Guijie Liang, Hongjun Yang, Mu Yao, Quasi-solid-state dye-sensitized solar cells based on gel electrolytes containing different alkali metal iodide salts, Solid State Ionics. 179 (2008) 2027-2030.

[24] P. Ma, Y. Fang, N. Fu, X. Zhou, S. Fang, Y. Lin, Ionic conductivity enhancement of “soggy sand” electrolytes with AlOOH nanofibers for dye-sensitized solar cells, Electrochimica Acta. 337 (2020) 135849.

View Article Online
DOI: 10.1039/D0CP01547D

[25] A. Scalia, F. Bella, A. Lamberti, C. Gerbaldi, E. Tresso, Innovative multipolymer electrolyte membrane designed by oxygen inhibited UV-crosslinking enables solid-state in plane integration of energy conversion and storage devices, Energy. 166 (2019) 789-795.

[26] F. Bella, S. Galliano, G. Piana, G. Giacona, G. Viscardi, M. Grätzel, C. Barolo, C. Gerbaldi, Boosting the efficiency of aqueous solar cells: A photoelectrochemical estimation on the effectiveness of $TiCl_4$ treatment, Electrochimica Acta. 302 (2019) 31-37.

[27] F. Bella, A. Sacco, G. Massaglia, A. Chiodoni, C. F. Pirri, M. Quaglio,. Dispelling clichés at the nanoscale: the true effect of polymer electrolytes on the performance of dye-sensitized solar cells, Nanoscale. 7(28) (2015) 12010-12017.

[28] I. P. Liu, L. W. Wang, Y. Y. Chen, Y. S. Cho, H. Teng, Y. L. Lee, Performance Enhancement of Dye-Sensitized Solar Cells by Utilizing Carbon Nanotubes as an Electrolyte Treating Agent, ACS Sustainable Chem. Eng. 8-2 (2020), 1102-1111.

[29] J. Ping, Hongbing Pan, Ping− Ping Hou, Meng-Yao Zhang, Xing Wang, Chao Wang, Jitao Chen, Decheng Wu, Zhihao Shen, Xing-He Fan, Solid polymer electrolytes with excellent high-temperature properties based on brush block copolymers having rigid side chains, ACS applied materials & interfaces. 9 (2017) 6130-6137.

[30] M. A. K. L. Dissanayake, C. A. Thotawatthage, G. S. K. Senadeera, T. M. W. J. Bandara, W. J. M. J. S. R. Jayasundera, B. E.Mellander, Efficiency enhancement by mixed cation effect in dye-sensitized solar cells with PAN based gel polymer electrolyte, Journal of Photochemistry and Photobiology A: Chemistry. 246 (2012) 29-35.

[31] T. M. W. J. Bandara, W. J. M. J. S. R. Jayasundara, M. A. K. L. Dissanayake, Maurizio Furlani, Ingvar Albinsson, B-E. Mellander, Effect of cation size on the performance of dye sensitized nanocrystalline TiO_2 solar cells based on quasi-solid state PAN electrolytes containing quaternary ammonium iodides, Electrochimica Acta. 109 (2013) 609-616.

[32] T. M. W. J. Bandara, M. A. K. L. Dissanayake, W. J. M. J. S. R. Jayasundara, Ingvar Albinsson, B-E. Mellander, Efficiency enhancement in dye sensitized solar cells using

View Article Online
DOI: 10.1039/D0CP01547D

gel polymer electrolytes based on a tetrahexylammonium iodide and MgI_2 binary iodide system, Physical Chemistry Chemical Physics. 14 (2012) 8620-8627.

[33] T. M. W. J. Bandara, H. D. N. S. Fernando, M. Furlani, I. Albinsson, M. A. K. L. Dissanayake, B-E. Mellander, Performance enhancers for gel polymer electrolytes based on LiI and RbI for quasi-solid-state dye sensitized solar cells, RSC Advances. 6 (2016) 103683-103691.

[34] C. W. Kuo, C. W. Huang, B. K. Chen, W. B. Li, P. R. Chen, T. H. Ho, C. G. Tseng, T. Y. Wu, Enhanced Ionic Conductivity in PAN-PEGME-LiClO4-PC Composite Polymer Electrolytes, Int J Electrochem Sci. 8 (2013) 3834-3850.

[35] D. Golodnitsky, E. Strauss, E. Peled, and S. Greenbaum. "On order and disorder in polymer electrolytes, Journal of The Electrochemical Society 162, no. 14 (2015) A2551-A2566.

[36] D. P. Almond, G. K. Duncan, A. R. West, The determination of hopping rates and carrier concentrations in ionic conductors by a new analysis of ac conductivity. *Solid State Ionics*, *8*(2), (1983) 159-164.

[37] N. Shukla, Awalendra K. Thakur, Archana Shukla, David T. Marx, Ion conduction mechanism in solid polymer electrolyte: an applicability of almond-west formalism, Int J Electrochem Sci. 9 (2014) 7644-7659.

[38] D. K. Pradhan, R. N. P. Choudhary, B. K. Samantaray, Studies of dielectric relaxation and AC conductivity behavior of plasticized polymer nanocomposite electrolytes, Int J Electrochem Sci. 3 (2008) 597-608.

[39] Y. Liu, A. Hagfeldt, X. R. Xiao and S. E. Lindquist, Investigation of influence of redox specie on the interfacial energetics of a dye-sensitized nanoporous TiO_2 solar cell, Sol Energy Mater Sol Cells. 55 (1998) 267–281.

[40] G. Redmond, D. Fitzmaurice, Spectroscopic determination of flatband potentials for polycrystalline titania electrodes in nonaqueous solvents. J Phys Chem. 97 (1993) 1426.

[41] B. Enright, G. Redmond, D. Fitzmaurice, Spectroscopic determination of flatband potentials for polycrystalline TiO2 electrodes in mixed solvent systems. J Phys Chem. 98 (1994) 6195.

View Article Online
DOI: 10.1039/D0CP01547D

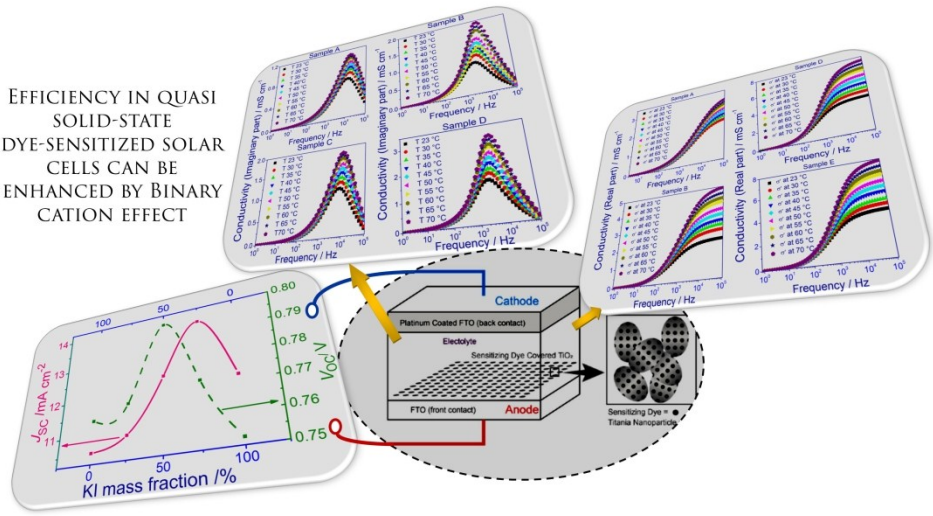

1222x1222mm (72 x 72 DPI)